Macromolecules

Article

pubs.acs.org/Macromolecules

Influence of Charged Groups on the Structure of Microgel and Volume Phase Transition by Dielectric Analysis

Wenjuan Su,[†,#] Man Yang,[†,#] Kongshuang Zhao,[*,†] and To Ngai[‡]

[†]College of Chemistry, Beijing Normal University, Beijing 100875, China

[‡]Department of Chemistry, The Chinese University of Hong Kong, Shatin, N. T. Hong Kong, China

ABSTRACT: The thermally sensitive charged poly(*N*-isopropylacrylamide-*co*-methacrylic acid) (P(NIPAM-*co*-MAA)) spherical microgel was prepared and their temperature-dependent volume phase transition behavior was systematically studied by analyzing the dielectric spectroscopy theoretically over a frequency range from 40 Hz to 110 MHz. It was found that the dielectric relaxation of the charged P(NIPAM-*co*-MAA) microgel drastically changed between 30 and 35 °C, and was significantly different from that of neutral PNIPAM microgels recently published in *Soft Matter*. The relaxation mechanism was speculated and the relaxation parameters were fitted after successfully eliminating the electrode polarization at low-frequency. On the basis of this, the differences in the structure, swelling ability and dehydration dynamics between charged P(NIPAM-*co*-MAA) and neutral PNIPAM microgels were compared. Although both of the two microgels showed the same changing trend around the volume phase transition temperature (VPTT), VPTT of charged P(NIPAM-*co*-MAA) microgels is less markedly than that of neutral PNIPAM. This suggests that the interaction between the PNIPAM chains and the solvent was changed significantly because of the introduction of charged groups. The volume phase transition behavior of P(NIPAM-*co*-MAA) microgels controlled by a delicate balance between the hydrophobic attraction of NIPAM and the electrostatic repulsion of the carboxylate group of methacrylic acid (MAA). These interactions are the essential reasons of the changes of the charged microgels in structure, swelling ability, and dehydration dynamics.

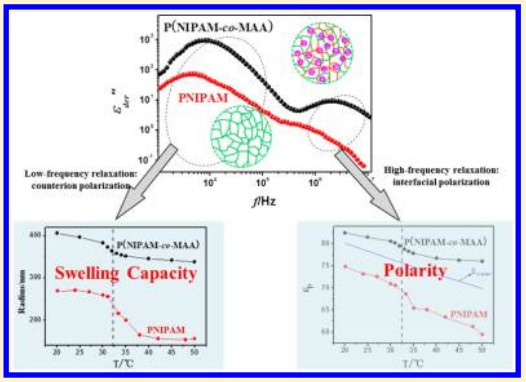

1. INTRODUCTION

Microgels are cross-linked polymer latex particles, and some of them will undergo a volume phase transition induced by temperature, pH, pressure, ionic strength, electric and magnetic fields. This kind of responsive microgels offers promising application in many fields, such as drug release, biosensors, chemical separation, and nanoreactors.[1,2] In these applications, the controlling of the swelling/deswelling of the microgels has been one of the concerned issues, because it involves the design of complex systems for specific applications.

Poly(*N*-isopropylacrylamide) (PNIPAM) is a well-known thermosensitive microgel system, which exhibits a significant volume phase transition above the lower critical solution temperature (LCST), around 32 °C in aqueous media.[3,4] Therefore, the transition temperature is also called the volume phase transition temperature (VPTT). The volume phase transition of PNIPAM microgels has been extensively investigated,[4−6] not only because of its strong application background, but also its significant implications in a number of living phenomena, especially the protein folding and DNA packing.[7,8] This is all because of its anatomical features: the PNIPAM microgel contains both hydrophilic amide groups and hydrophobic hydrocarbon chains. It is well-known that the volume phase transition is determined by the hydrophobic interactions within the PNIPAM molecule.[9] On the other hand, many studies have shown that the VPTT can be modified by additives of inorganic salt,[10−12] surfactants,[7,13,14] ionic liquid,[15−17] alcohol,[18,19] and urea.[8,20] Besides that, the VPTT and swelling/deswelling behavior are also controlled by the introduction of charged groups (e.g., carboxyl, sulfonic, and amino group) to PNIPAM microgel networks. For example, the result of Wu[21] indicates that the VPTT of poly(*N*-isopropylacrylamide-*co*-acrylic acid) P(NIPAM-*co*-AA) hydrogel is slightly higher than that of PNIPAM. In other words, the charge density within the PNIPAM network may affect the VPTT of P(NIPAM-*co*-MAA) microgel and its dynamic or rheological properties.[22−24]

For neutral PNIPAM microgels, the VPTT is mainly determined by the two competed interaction: hydrogen bonding interaction and hydrophobic interaction,[9,25] and for charged P(NIPAM-*co*-MAA) microgel, there is an extra osmotic pressure from ion/solvent mixing and electrostatic effects, which will also contribute to the swelling of the microgel.[26] Therefore, the volume phase transition of the charged P(NIPAM-*co*-MAA) microgel is the result of three competed interactions: the hydrogen bonding between the amide groups

Received: April 18, 2016
Revised: September 9, 2016
Published: October 7, 2016

DOI: 10.1021/acs.macromol.6b00809
Macromolecules 2016, 49, 7997−8008

of NIPAM and water molecules, the electrostatic repulsion of the carboxylate group of MAA, and the hydrophobic interaction of the pendent isopropyl groups as well as that of the backbone of NIPAM monomers. Furthermore, the effective charge density of microgel depends not only on the amount of charged groups but also on the pH and the ionic strength of solutions, which makes the relationship between volume phase transition and effective charge density more complex. For charged P(NIPAM-*co*-MAA) microgel, some studies have shown that the volume phase transition becomes discontinuous with increasing amount of charged groups.[23,27,28] However, some literatures gave opposite conclusion.[24,29,30] Unfortunately, the systematic investigations on the properties of charged P(NIPAM-*co*-MAA) microgel suspension and even the structural evolution and dehydration dynamics during volume phase transition are still scarce. Thus, far, the effect of charged groups on the microscopic mechanism of the transition is ambiguous and poorly understood.

To explore and solve the above problems, in the present work, dielectric relaxation spectroscopy was employed to study the volume phase transition behaviors of charged (P(NIPAM-*co*-MAA)) microgel. Dielectric spectroscopy has been continually used to study the volume phase transition of PNIPAM microgels,[31−34] including our own recent research.[35] These researches have shown that dielectric spectroscopy is a promising tool to investigate the internal morphology and thermal behavior of thermally sensitive microgel system. On the basis of the appropriate physical model, abundant information about counterion movement, interaction (hydrogen bond and electrostatic interaction), dehydration dynamics, and electrical properties of P(NIPAM-*co*-MAA) microgel can be obtained. In addition, to understand how the charged groups affect the hydrophilic-to-hydrophobic phase transition, we systematically compared the result of charged P(NIPAM-*co*-MAA) microgel to that of the neutral PNIPAM microgels published recently.[35]

2. EXPERIMENTAL SECTION

2.1. Materials and Preparation of the Sample. *Materials.* *N*-Isopropylacrylamide (NIPAM, Fluka) was recrystallized using a 1:1 toluene−*n*-hexane mixture twice. Methacrylic acid (MAA, Merck) was vacuum distilled at 50 °C to remove the stabilizer. *N*,*N*′-Methylenebis-(acrylamide) (MBA, Fluka) was recrystallized by using methanol, and potassium persulfate (KPS, Merck) was used as received. Deionized water was used in all the experiments.

Preparation of Microgels. PNIPAM-based microgels were prepared by surfactant-free precipitation polymerization, based on NIPAM as a monomer, MBA as a cross-linker, and KPS as a initiator. We have synthesized two types of nanometer-sized microgels: (a) an uncharged PNIPAM microgel (no comonomer) (essentially it is slightly charged because a tiny amount of charge is inevitable during the preparation process) and (b) a charged P(NIPAM-*co*-MAA) microgel (MAA as the comonomer), as shown in Figure 1. Because the polymerization reaction is based on a semibatch and temperature-programmed operation,[36] the resultant microgels have a homogeneous spatial distribution of cross-linking density and charge density.

Figure 1. Schematic of (a) neutral PNIPAM microgel and (b) charged P(NIPAM-*co*-MAA) microgel in a swollen state.

Charged P(NIPAM-co-MAA) Microgels. First, 0.9 g of NIPAM monomer was dissolved in 45 mL of deionized water and filtered to remove any solid impurities, and then it was preheated to 40 °C and purged with nitrogen gas for 1 h to remove the dissolved oxygen. After that, 0.05 g of KPS was dissolved in 1 mL of deionized water and added to the reaction vessel to initiate the polymerization. Two minutes after the initiation, 5 mL of solution containing 0.3 g of NIPAM, 0.03 g of MBA, and 0.15 mL of MAA was added within 1 h using a syringe pump. When the reaction mixture started to turn opalescent, the temperature was ramped to 70 °C in 1 h. After all of the 5 mL comonomer solution was added, the reaction mixture was stirred for 2 h more at 70 °C.

Neutral PNIPAM Microgel. The preparation for neutral PNIPAM microgels synthesis was done similarly to that of P(NIPAM-*co*-MAA) microgels. The only difference is that the 0.15 mL of MAA was not added into the polymerization reaction. During the preparation process, though no extra charge carriers were added, a tiny amount of charge in the PNIPAM microgel is inevitable during the preparation of microgels (e.g., from the initiator KPS). Therefore, tiny amounts of charge also exist in PNIPAM microgel, but the charge amount in PNIPAM microgel is uncertain and far less than that in P(NIPAM-*co*-MAA) microgel.

2.2. Methods. *Dynamic Light Scattering (DLS).* For a first characterization of the swelling/deswelling behaviors of PNIPAM and P(NIPAM-*co*-MAA) microgel particles, DLS measurements were conducted using a modified commercial light-scattering spectrometer equipped with an ALV-5000 multi-τ-digital time correlator and a He−Ne laser, at temperatures from 25 to 50 °C.

Dielectric Relaxation Spectroscopy (DRS). Dielectric measurements of PNIPAM-based microgels were carried out using a 4294A precision impedance analyzer (Agilent Technologies) in a frequency range from 40 Hz to 110 MHz at temperatures from 20 to 50 °C. A dielectric measuring cell with concentrically cylindrical platinum electrodes was employed to load the samples, the effective area of the electrodes was 78.5 mm^2, and the electrode distance was 8 mm. The temperature of the samples was controlled by a circulating thermostated water jacket. The applied alternating field was 500 mV. All the experimental data were corrected for errors arising from stray capacitance (C_r), cell constant (C_l), and residual inductance (L_r) by Schwan method.[37,38] They are 0.09 pF, 0.72 pF, and 2.29 nH, respectively, determined with three standard substances (pure water, ethanol and air) and KCl solution of varying concentrations. Then the corrected data of capacitance C_s and conductance G_s at each frequency were converted to permittivity and conductivity by equations $\varepsilon = C_s/C_l$ and $\kappa = G_s\varepsilon_0/C_l$ (ε_0 is the permittivity of vacuum).

2.3. Determination of Relaxation Parameters. The dielectric response of PNIPAM-based microgels suspension in an applied electric field with angular frequency ω (= $2\pi f$, f is the measurement frequency) can be characterized by the complex permittivity ε^* which is defined as[39]

$$\varepsilon^*(\omega) = \varepsilon - j\varepsilon'' = \varepsilon - j\frac{\kappa - \kappa_l}{\omega\varepsilon_0} \quad (1)$$

where ε and κ are the frequency-dependent permittivity and complex conductivity of the system, respectively. ε'' is the dielectric loss, and $j = (-1)^{1/2}$. κ_l is the low-frequency limit of conductivity (namely the low-frequency conductivity or dc conductivity), which was read out from the conductivity spectra at low frequency.

In our investigated frequency window, no matter for neutral PNIPAM microgels suspension, or for charged P(NIPAM-*co*-MAA) microgels suspension, the measured dielectric spectra at each temperature shows two remarkable relaxations and electrode polarization that is annoying but unavoidable. Therefore, the following relaxation function including two Cole−Cole's terms and the electrode polarization term $A\omega^{-m}$ (A and m are adjustable parameters) was employed to analyze the experimental spectra:[40]

DOI: 10.1021/acs.macromol.6b00809
Macromolecules 2016, 49, 7997−8008

$$\varepsilon^* = \varepsilon_h + \sum_i \frac{\Delta\varepsilon_i}{1 + (j\omega\tau_i)^{\beta_i}} + A\omega^{-m} \quad (2)$$

where ε_h is the high frequency limit of permittivity, i is the number of dielectric relaxations (i = 1, 2 in this work); $\Delta\varepsilon_i$ and τ_i (= $1/2\pi f_{0i}$, f_{0i} is the characteristic relaxation frequency) are the dielectric increment and relaxation time, respectively; β_i ($0 < \beta_i \leq 1$) is the Cole−Cole parameter indicating the distribution of the relaxation time.

In order to determine the characteristic frequency clearly, the derivative dielectric loss ε''_{der} is presented on the basis of the logarithmic derivative of raw ε:[41,42]

$$\varepsilon''_{der}(\omega) = -\frac{\pi}{2}\frac{\partial\varepsilon}{\partial \ln \omega} \approx \varepsilon''_{Rel}(\omega) \quad (3)$$

The logarithmic derivative method proves to be effective in separating relaxations from the EP effect and offers a good way to resolve overlapping relaxation peaks due to peak sharpening. By introducing the real part of eq 2 into the derivative expression eq 3, we get the following expression:

$$\varepsilon''_{der}(\omega) = \frac{\pi}{2}\left(\sum_i \frac{\beta_i(\Delta\varepsilon_i)(\omega\tau_1)^{\beta_i}\cos\left[\frac{\beta_i\pi}{2} - (1+\beta_i)\theta_i\right]}{1 + 2(\omega\tau_i)^{\beta_i}\cos\frac{\beta_i\pi}{2} + (\omega\tau_i)^{2\beta_i}}\right) + Am\omega^{-m} \quad (4)$$

where $\theta_i = \arctan\left[\sin(\beta_i\pi/2)/((\omega\tau_i)^{-\beta}{}_i + \cos(\beta_i\pi/2))\right]$. eq 4 has the same set of variables as that in eq 2 and was used to fit the derivative dielectric loss curve in this work.

Figure 2 shows a representative dielectric spectra of $\varepsilon(f)$ and derivative $\varepsilon''_{der}(f)$ of P(NIPAM-*co*-MAA) microgels suspension at 30 °C. Two relaxation processes, named relaxation-1 and relaxation-2 for the low- and high-frequency relaxation respectively, were clearly observed although the electrode polarization (EP) effect covers the low-frequency partly below about 3 kHz. It is obvious that the low-frequency relaxation of 10 kHz was clearly separated from the high-frequency relaxation. The low- and high- frequency relaxations are all depended on whether the microgels are charged, and are little influenced by the temperature of the microgel microsphere suspension which can be seen in Figure 4b. The two relaxations were well represented by eqs 2 and 4. The relaxation parameters in Table 1 are obtained by fitting the eq 4 to the observed dielectric spectra.

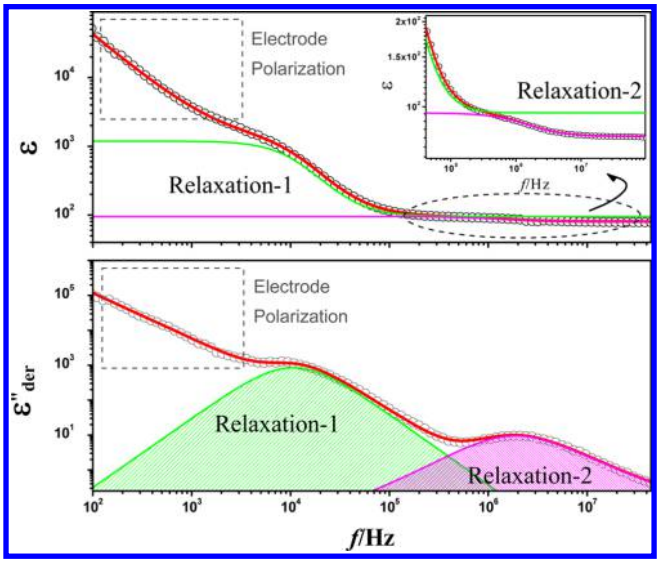

Figure 2. Frequency dependence of the relative permittivity (above) and the derivative dielectric loss (below) of P(NIPAM-*co*-MAA) microgels suspension at 30 °C. The hollow circles represent the experiment results, and the solid lines represent the best fitting.

Table 1. Relaxation Parameters of P(NIPAM-*co*-MAA) Microgels Suspension of Various Temperatures

T/°C	ε_h	$\Delta\varepsilon_1$	$\Delta\varepsilon_2$	β_1	β_2	τ_1/μs	τ_2/ns
20	82.5	1044.4	16.5	0.98	0.98	17.7	128.3
25	81.3	1046.5	16.2	0.98	0.91	16.9	124.3
30	80.2	1050.4	15.7	0.98	0.98	15.8	116.6
31	79.4	1053.3	15.4	0.97	0.93	14.9	107.4
32	78.9	1057.4	14.6	0.97	0.92	14.3	99.2
33	78.6	1064.6	13.9	0.97	0.92	13.8	87.9
34	78.3	1075.9	13.4	0.97	0.93	13.5	83.8
35	78.2	1085.5	13.1	0.99	0.95	13.3	81.0
40	77.3	1094.8	12.5	0.94	0.94	12.9	75.5
45	75.8	1099.5	12.2	0.98	0.96	12.6	73.9
50	74.9	1103.2	12.1	0.98	0.99	12.3	72.5

3. RESULTS AND DISCUSSION

3.1. Swelling/Deswelling Behaviors of Microgels. Figure 3 shows the temperature dependence of the hydrodynamic radius R_h of neutral PNIPAM and charged P(NIPAM-*co*-MAA) microgels. Both of the two microgel suspensions demonstrate the typical thermosensitive behavior: R_h decreases with the increase of temperature and abruptly decreases at about 32.5 °C (i.e., VPTT). Moreover, the VPTT is nearly in the same temperature range regardless of whether or not the microgel is charged. However, the swelling/deswelling behaviors of these two types of microgels are quite different: compared with neutral PNIPAM microgels, the charged P(NIPAM-*co*-MAA) microgels exhibited a greater ability to swell and have undergone a less sharp volume phase transition. Such difference is due to the charges introduced onto the microgels and the resulting extra osmotic pressure and interactions.

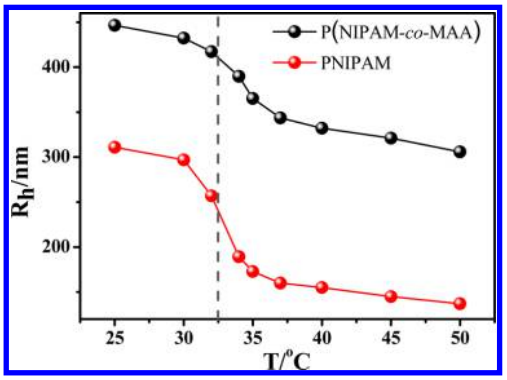

Figure 3. Temperature dependence of the mean hydrodynamic radius for PNIPAM (red) and P(NIPAM-*co*-MAA) (black) microgels. The VPTT is indicated by a dashed vertical line.

3.2. Dielectric Behavior of PNIPAM-Based Microgels Suspension. Figure 4 shows the three-dimensional representations for the temperature dependence of the dielectric loss spectra ($\varepsilon''_{der} - f$) for both neutral PNIPAM and charged P(NIPAM-*co*-MAA) microgels suspension in the temperature range of 20 to 55 °C. They are obtained according to the method in section 2.3. The insets of Figure 4 are the two-dimensional diagrams cut at the temperatures before (black curve) and after (red curve) the VPTT. It is clear from Figure 4 that two remarkable dielectric relaxations were observed at around 10^4 Hz and 10^6 Hz for both of the two suspensions, i.e. low- and high-frequency relaxation as mentioned before.

DOI: 10.1021/acs.macromol.6b00809
Macromolecules 2016, 49, 7997−8008

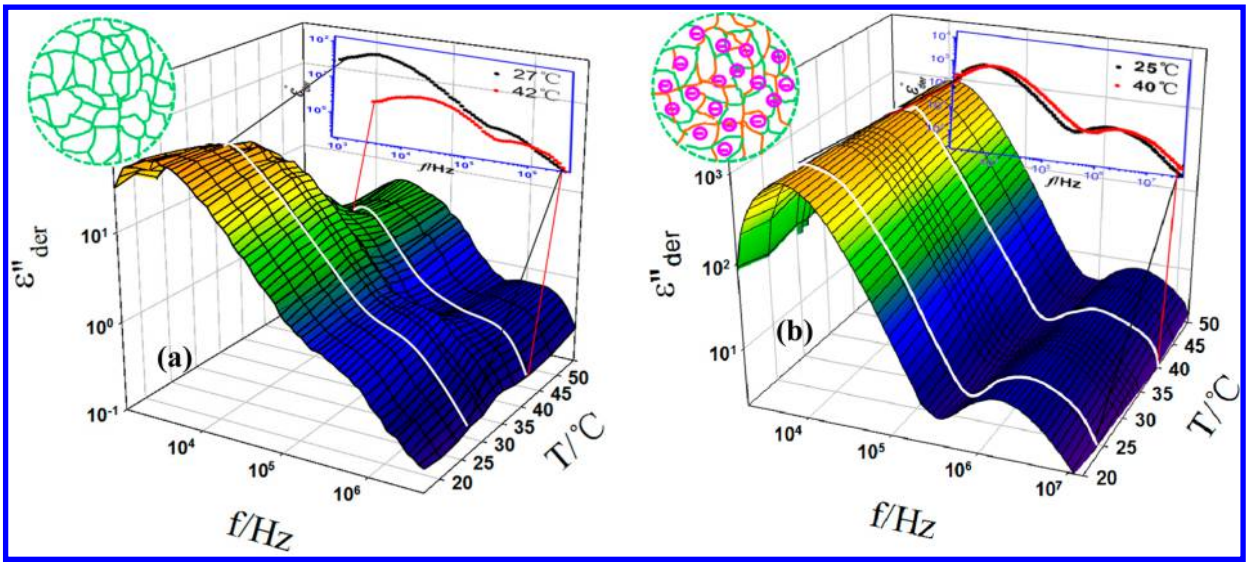

Figure 4. Derivative dielectric loss versus frequency and temperature in three-dimensional representations for (a) neutral PNIPAM microgels and (b) P(NIPAM-*co*-MAA) microgels suspension. The inset shows the change of dielectric loss spectra above and below the VPTT.

Moreover, their low-frequency relaxation strengths are much larger than that of the high-frequency relaxation, indicating they are similar in the dielectric behavior. However, it is very obvious that the temperature dependence of dielectric spectrum strongly depends on the charges of microgel as can be seen clearly in Figure 4.

3.3. Dielectric Relaxation Analysis of Microgels Suspension. To accurately characterize the two relaxation processes and investigate the effect of charged groups on volume phase transition, it is necessary to determine the relaxation parameters, i.e. the dielectric increments ($\Delta\varepsilon_1 = \varepsilon_l - \varepsilon_m$ and $\Delta\varepsilon_2 = \varepsilon_m - \varepsilon_h$ (where the subscripts l, m, and h denote the low, medium, and high frequency limit values, respectively)) and relaxation times (τ_1 and τ_2) of low- and high-frequency relaxation, respectively. The relaxation parameters of the P(NIPAM-*co*-MAA) microgels suspensions between 20 and 50 °C were obtained by fitting eq 4 including two Cole−Cole's terms to the dielectric spectrum and listed in Table 1.

3.3.1. Relaxation Mechanisms. 3.3.1.1. Relaxation Mechanisms of P(NIPAM-co-MAA) Microgel Suspension. On the basis of the dielectric theory of aqueous colloidal systems[43] and our previous research on neutral PNIPAM microgels,[35] we speculate the low-frequency relaxation was caused by the "counterion polarization" which is due to the asymmetry of microgel with respect to the ion sign, and the high-frequency relaxation arises from the "interfacial polarization" of microgel/water. Besides, considering that the anionic electric charges on the polymer chains are not not only localized on the surface of microgels but also exist in the interior of microgels, the counterion polarization inside the microgel also contributes to the high frequency relaxation.

3.3.1.1.1. Low-Frequency Relaxation: Counterion Polarization. When the counterions in electrical double layer (EDL) transport from one side of a spherical particle to the other side under an applied electric field, counterion polarization occurs, which is often observed as a lower frequency relaxation.[43] In this work, the relaxation time τ_1 of the low-frequency relaxation is controlled by the radius a of the microgel particle, and the relationship between τ_1 and a can be described as

$$\tau_1 \approx \frac{a^2}{D} \tag{5}$$

where D is the diffusion coefficient and it increases by 2−3% per degree as the temperature increases from 25 °C.[44] In our case of P(NIPAM-*co*-MAA) microgels suspension, the counterions are mostly hydrogen ions (H^+) which were from the dissociation of comonomer MAA. Thus, the radius a of microgel particle of P(NIPAM-*co*-MAA) at different temperatures was estimated according to eq 5 from τ_1 in Table 1 and diffusion coefficient of hydrogen ion D_{H^+}(=9.3 × 10^{-5} cm^2 s^{-1} at 25 °C). The temperature dependence of the radius a of P(NIPAM-*co*-MAA) microgel is shown in Figure 5 by the black

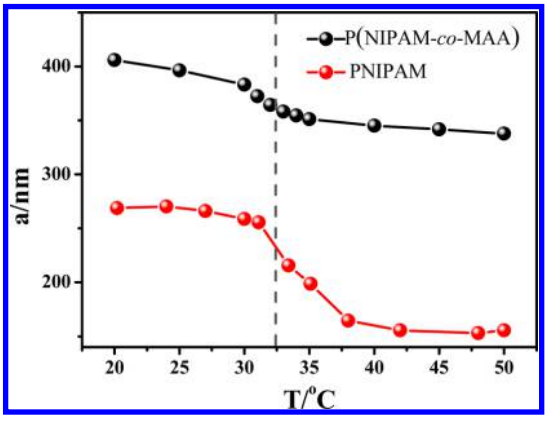

Figure 5. Temperature dependence of the radius of two types of microgel particles, estimated based on the theory of counterion polarization. The red data of PNIPAM microgel were from our recently published work.[35]

curve. The red curve for PNIPAM microgel in Figure 5 is from ref 35. It is important to remember that these estimates are remarkably in agreement with the measurement results by DLS (see Figure 3). This suggests that the reduction of τ_1 correlated significantly with the decrease in the microgel particle's size upon shrinking. And it also proved that the low-frequency relaxation of both P(NIPAM-*co*-MAA) and PNIPAM is caused by the counterion polarization around the microgel particle.

DOI: 10.1021/acs.macromol.6b00809
Macromolecules 2016, 49, 7997−8008

3.3.1.1.2. High-Frequency Relaxation: Interfacial Polarization Effect of Counterions. Compared to slower counterion polarization mode at low frequencies, the interface polarization, which is ascribed to the accumulation of charges in the electrolyte layer adjacent to the particle surface whose thickness is of the order of EDL thickness, occurs at higher radio frequency range (typically in the range of MHz) because the space charges lead to a larger macro dipole moment which response extra electric field much slower than the dipole orientation of molecule but faster than the counterion migration in EDL. The relaxation time of interfacial polarization, corresponding to the time needed for ions to diffuse a distance of the order of EDL thickness, can be roughly estimated by the well-known Einstein equation,[45]

$$\tau_2 \approx \frac{\chi_D^{\,2}}{D} \tag{6}$$

and χ_D is a measure of the EDL thickness, which is also known as the Debye length characterizing the size of the diffuse ion cloud, defined as

$$\chi_D = \sqrt{\frac{\varepsilon_a \varepsilon_0 k_B T}{e^2 \sum_i C_i Z_i^{\,2}}} \tag{7}$$

where e, C, and Z are the elementary charge, ion concentration, and the valence of ion, respectively. χ_D was estimated using eq 6, with τ_2 obtained experimentally (see Table 1) and D_{H^+}. A reasonable thickness of EDL whose value is only decades of nanometers (far less than the radius of the microgels as shown in Figure 3) was obtained, which demonstrated that the high-frequency relaxation is caused by the interfacial polarization.

The relaxation behavior of charged microgel, is essentially similar to that of polyelectrolyte. The ion movement parallel and perpendicular to the polymer chain also contributes to the relaxations. Therefore, besides the counterion movement in the EDL of the microgel surface, one should also consider the ions movement inside the microgel. Counterion motion perpendicular to the polymer chains would be observed at the relaxation time calculated by eq 6. That is to say, the interfacial polarization effect of counterion inside the microgel also contributes to the high-frequency relaxation. But along with the collapse of the microgel, due to the shortened distance between the polymer chains, the motion distance of the counterion will also become shorter, as the motion scale of counterion perpendicular to the chains is approximately equal to the correlation length (i.e., interchain distance).[46,47] Since the relaxation intensity of interfacial polarization for counterions inside microgel is proportional to the motion distance of counterion.[46] Therefore, the relaxation of the collapsed microgel is mainly dominated by the diffusion of counterions on the surface of microgel, which are relatively less restricted compared with those inside the microgel.

3.3.1.2. Relaxation Mechanisms of PNIPAM Microgel Suspension. 3.3.1.2.1. Low-Frequency Relaxation: Counterion Polarization. As proved in the above section, the low-frequency relaxation of PNIPAM microgel is the same as P(NIPAM-*co*-MAA) microgel, i.e., counterion polarization.

3.3.1.2.2. High-Frequency Relaxation: Interfacial Polarization and Side Chain Motions. In the preparation of PNIPAM microgel, due to the introduction of initiator KPS, tiny amounts of charge also exist in PNIPAM microgel. Therefore, interfacial polarization may also contributes to the high-frequency relaxation of PNIPAM, qualitatively similar to P(NIPAM-*co*-MAA). Considering that the number of fixed charge in PNIPAM is much less than that of P(NIPAM-*co*-MAA), and that most of them are located on the surface of the microgel due to the hydrophilic interaction, the number of fixed charges and counterions inside microgel is much smaller as compared to that of P(NIPAM-*co*-MAA). Therefore, the polarization of electric double layer surrounding polymer chains inside the microgel could be negligible and only that on the surface of the microgel is taken into account here.

Figure 6 is a comparison of the dielectric increment of high-frequency relaxation for PNIPAM and P(NIPAM-*co*-MAA)

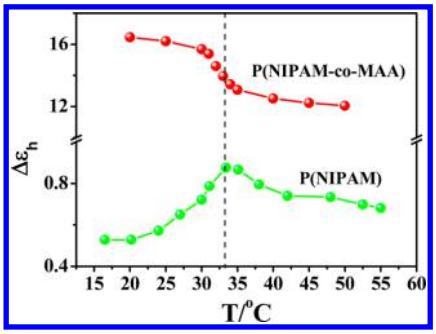

Figure 6. Temperature dependence of dielectric increment of high-frequency relaxation for PNIPAM and P(NIPAM-*co*-MAA) microgels.

microgel. It is clearly seen that the high-frequency dielectric increment of PNIPAM suspension is much smaller than that of P(NIPAM-*co*-MAA) suspension (nearly two orders smaller in magnitude). Since the relaxation strength of interfacial polarization is related to the difference in electrical properties between disperse phase and medium ($\Delta\varepsilon = 9p(\varepsilon_a\kappa_p - \varepsilon_p\kappa_a)^2/[(2\kappa_a + \kappa_p)^2(2\varepsilon_a + \varepsilon_p)]$. The subscript p denotes microgel and a denotes the medium water),[48] as the difference in electrical properties between PNIPAM and water is not very obvious (the difference between κ_p/ε_p and κ_a/ε_a is very small), the dielectric increment is smaller; while for the P(NIPAM-*co*-MAA) suspension, although the permittivity of microgel is nearly equal to aqueous phase, due to a large number of fixed charge in microgel, the conductivity of P(NIPAM-*co*-MAA) microgel is far greater than the conductivity of the aqueous phase, which leads to a greater dielectric increment.

Besides, the variation tendency of relaxation intensity vs temperature of PNIPAM is obviously different from that of P(NIPAM-*co*-MAA), and a peak occurs at about 32 °C. This suggests that, in addition to the contribution of the interfacial polarization, other mechanisms may also contribute to the high-frequency relaxation. One possible mechanism is the motion of side chain which is closely associated with the hydrogen bonds as confirmed by several researchers.[49,50] Below VPTT, the motion of solvated side chains is constrained by the hydrogen bond of amide group-water and the hydrogen bond bridges between side chains[51] (darker shadow in Figure 7a). However, as the temperature increases part of hydrogen bonds fracture and the constraint weakens, thus the dielectric increment of side chain relaxation should increase with temperature. Above VPTT, with the collapse of PNIPAM microgel, side chain motion is greatly limited because of the formation of hydrogen bonds between side chains (Figure 7b), and the contribution of side chain relaxation is significantly reduced.

As explained above, due to the tiny difference in the electrical properties of PNIPAM and aqueous phase, the relaxation

DOI: 10.1021/acs.macromol.6b00809
Macromolecules 2016, 49, 7997−8008

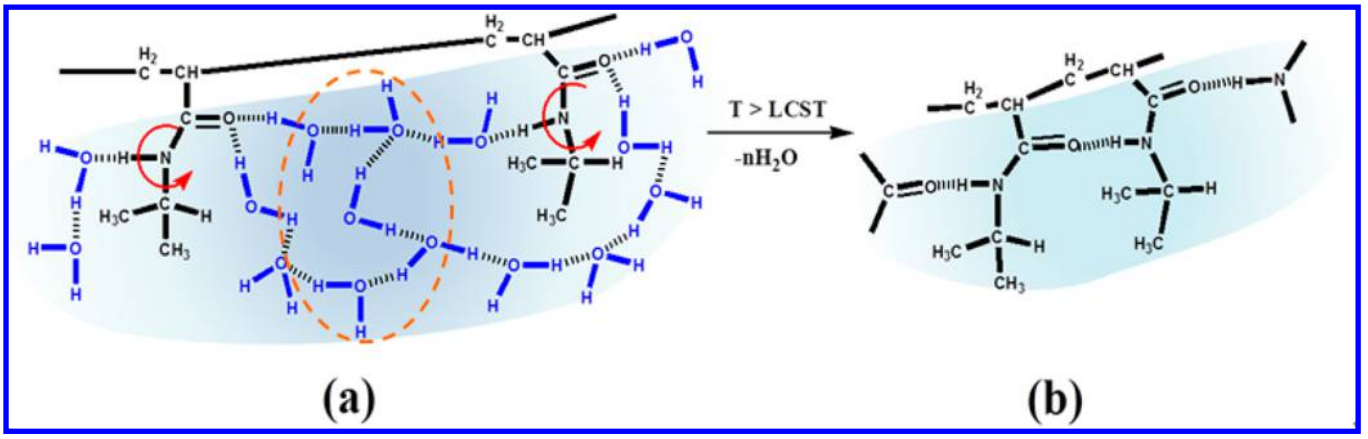

Figure 7. Schematic of the local chain motions inside the PNIPAM microgels: (a) below VPTT, the PNIPAM chain is constrained due to hydrogen bonds of amide group−water and hydrogen bond bridges between side chains; (b) above VPTT, the conformation of PNIPAM microgel becomes more compact due to hydrogen bond between side chains. The red arrows represent the motion of side chains.

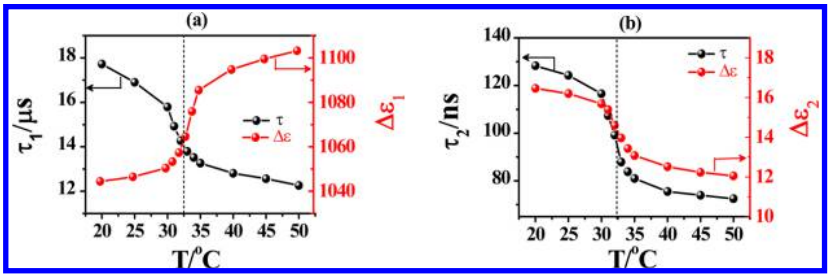

Figure 8. Temperature dependence of dielectric increment (above) and relaxation time (below) for (a) low- and (b) high-frequency relaxation.

strength of interfacial polarization for PNIPAM is small. In spite of this, the interfacial polarization still contributes to the high-frequency relaxation in the whole temperature range, and the variation tendency of relaxation strength of PNIPAM should be similar to that of P(NIPAM-*co*-MAA). As shown in Figure 6, At T < VPTT, the high-frequency relaxation increment of PNIPAM increases with temperature, which means that the polarization side chain relaxation may be dominant in this tempertaure range. And for the highly swollen PNIPAM (T < VPTT), although PNIPAM microgel is weakly charged, its interior contains large amounts of water in the swollen state, so the difference between the dielectric properties of PNIPAM microgel and the solvent water is not obvious. Thus, interfacial polarization play a minor role at temperature below VPTT. At T > VPTT, the high-frequency relaxation increment decreases with temperature, which is in line with the variation tendency of interfacial polarization. At the same time, because the side chain relaxation is greatly reduced after the collapse of microgel as discussed above, we speculate that the interfacial polarization may play a leading role at temperature above VPTT.

That is to say, both the side chain relaxation and interfacial polarization contribute to the high-frequency relaxation of PNIPAM, but they are dominant at different temperature ranges, respectively. It should be noted that, interfacial polarization is not intrinsic to PNIPAM, but was unavoidable due to the difference in electrical property between microgel and medium[48] because of sample preparation procedure utilizing KPS.

3.3.2. The Volume Phase Transition Determined by Relaxation/Phase Parameters. Figure 8 shows the temperature dependence of the dielectric increment and the relaxation time of P(NIPAM-*co*-MAA) microgels suspension for the low- and high-frequency relaxations, respectively. It is obvious from Figure 8 that all the relaxation parameters ($\Delta\varepsilon_1$, τ_1, $\Delta\varepsilon_2$ and τ_2) exhibit significant changes at the same temperature of 32.5 °C, being completely consistent with the results by DLS (see Figure 3). We consider this temperature as the volume phase transition temperature (VPTT) of the charged P(NIPAM-*co*-MAA) microgels. In this sense, the volume phase transition behavior can be monitored effectively by the temperature dependence of dielectric relaxation parameters. Wu et al.[21] investigated P(NIPAM-*co*-AA) hydrogel by Fourier transform infrared spectroscopy (FT-IR) in combination with the perturbation correlation moving window (PCMW) technique and two-dimensional correlation spectroscopy (2Dcos), and they found that the VPTT of PNIPAM-*co*-AA is slightly higher than that of PNIPAM. This is different with the result in this work. This may be because that the PCMW can determine the exact volume phase transition point, while dielectric method is relatively mesoscopic, but is also effective for estimating roughly VPTT.

Moreover, the volume phase transition behavior of P(NIPAM-*co*-MAA) microgels was extremely well monitored by the temperature dependence of the phase parameters of the microgels suspension. To obtain more detailed information about the inner electrical properties of the charged P(NIPAM-*co*-MAA) microgel particle and its structure change when the microgels collapse, it is necessary to calculate the parameters of the constitute phase of microgel suspension. To this end, we regard the P(NIPAM-*co*-MAA) microgel suspension as a particle dispersion: with different dielectric properties, that is the microgel particles with radius a and complex permittivity ε_p^* ($= \varepsilon_p - j\kappa_p/\omega\varepsilon_0$) dispersed in a continuous aqueous medium

DOI: 10.1021/acs.macromol.6b00809
Macromolecules 2016, 49, 7997−8008

with complex permittivity ε_a^* (= $\varepsilon_a - j\kappa_a/\omega\varepsilon_0$) in a volume fraction ϕ. The complex permittivity of the whole suspension ε^* is given by Hanai's mixture equation, which is applicable to the concentrated suspension, as follows:[52]

$$\frac{\varepsilon^* - \varepsilon_p^*}{\varepsilon_a^* - \varepsilon_p^*}\left(\frac{\varepsilon_a^*}{\varepsilon^*}\right)^{1/3} = 1 - \phi \tag{8}$$

Here, the parameters of ε_p, κ_p, ϕ, and κ_a are relevant to the inner electrical parameters of the P(NIPAM-*co*-MAA) microgels suspension and are called the "phase parameters". Further, we calculated the phase parameters which are approximately related to the dielectric high-frequency relaxation parameters (ε_m, κ_m, ε_h) in Table 1 and κ_h by means of the dielectric model described above and a systematic numerical method(refer to literatures[52,53]). The calculated phase parameters of P(NIPAM-*co*-MAA) microgel are listed in Table 2. The phase parameters of PNIPAM microgel is from ref35.

Table 2. Phase Parameters of P(NIPAM-*co*-MAA) Microgel Suspensions at Various Temperatures

T/°C	ε_a[a]	κ_a (mS/m)	ϕ	ε_p	κ_p (mS/m)
20	80.1	0.7	0.978	82.5	4.2
25	78.3	0.8	0.969	81.4	4.6
30	76.5	0.9	0.956	80.5	5.1
31	76.2	1.0	0.941	80.2	5.2
32	75.8	1.1	0.920	79.4	5.3
33	75.5	1.2	0.883	78.7	5.5
34	75.1	1.3	0.854	78.3	5.6
35	74.8	1.4	0.837	77.8	5.7
40	73.1	1.5	0.821	76.7	6.2
45	71.5	1.7	0.819	76.2	6.7
50	69.9	1.8	0.817	76.0	7.2

[a] ε_a were estimated with the *Handbook of Chemistry and Physics*.[54]

3.4. Unique Properties of the Charged P(NIPAM-*co*-MAA) Microgels. As we all have observed in Figure 4, the temperature dependence of the dielectric spectrum of the charged P(NIPAM-*co*-MAA) microgels is largely different from that of the neutral PNIPAM microgels. Essentially, the reasons lie in the difference of structures and properties of these two types of microgels. In order to investigate the effect of charged groups on microgel structure and volume phase transition behavior, the above analyzing results of charged P(NIPAM-*co*-MAA) were systematically compared with those of neutral PNIPAM microgels published recently.[35]

3.4.1. Microgel Structure. Table 3 is a comparison of the dielectric relaxations characteristic between P(NIPAM-*co*-MAA) and PNIPAM microgel suspensions. The additional local chain motions at high frequency for PNIPAM microgel reveals that the chains in PNIPAM are more flexible than those in P(NIPAM-*co*-MAA), i.e., the network of the charged microgel is more rigid. The difference in rigidity is because that the introduced polar charged groups (MAA) not only increases the rotating barrier of polymer and the energy difference between different equilibrium conformation, but also generates strong interaction in the network, which reduces the flexibility of the polymer chains and hinder their movement.[55,56]

Table 3. Comparison of the Characteristic Dielectric Relaxations between P(NIPAM-*co*-MAA) and PNIPAM Microgel Suspensions

sample	low-frequency relaxation	high-frequency relaxation
PNIPAM	counterion polarization	interfacial polarization and local chain motions
P(NIPAM-*co*-MAA)	counterion polarization	interfacial polarization effect of counterion

Moreover, the difference between charged P(NIPAM-*co*-MAA) and neutral PNIPAM microgels was also detected by the change of phase parameters with temperature. Parts a and b of Figure 9 show the temperature dependence of the conductivity and the permittivity of the two PNIPAM-based microgel particles, respectively. (The data of PNIPAM microgel are taken from ref 35. Note that the data at T < VPTT for PNIPAM microgel are only for reference, because in this temperature range the high-frequency relaxation mainly contributes to side chain relaxation.) Because ionic monomer of MAA was introduced into the neutral PNIPAM microgel network and the microgel particles are electrically charged. Therefore, the conductivities of P(NIPAM-*co*-MAA) microgel particles are bigger than that of PNIPAM microgel particles at each temperature as shown in Figure 9a. The conductivity κ_p of P(NIPAM-*co*-MAA) microgel increased with temperature, implying the charge density increased as the cross-linked PNIPAM-*co*-MAA chains collapse to form a more compact microgel sphere. Inversely, the permittivity ε_p decreased with the increase of temperature, indicating that water molecules are gradually expelled from the microgels. Besides, both κ_p and ε_p for these two types of PNIPAM-based microgel exhibited significant changes at the same temperature of 32.5 °C (VPTT), indicating the phase transition occurs near this temperature.

More interestingly, in the experimental temperature range the permittivity of PNIPAM microgel is smaller than that of P(NIPAM-*co*-MAA) and larger than water at each temperature, that is ε_p(P(NIPAM − *co*-MAA)) > ε_a > ε_p(PNIPAM). It is well-known that water has a relatively large permittivity (ε_a = 78, 25 °C). Meanwhile, it should be noted that the microgel particles still retain more than 80% of water even in a highly collapsed state, as has been confirmed by DLS[4], so it is well accepted that the permittivity of PNIPAM microgel particles is always less than that of ε_a at each temperature and maintained at a higher values of 60−75. However, it seems a little incomprehensible that the permittivity of P(NIPAM-*co*-MAA) microgel particles is slightly larger than permittivity of water. It is generally accepted that two factors may lead to a larger permittivity: the cis−trans isomerism of molecules,[57] and the particular arrangement of water molecule in a confined environment.[57,58] For the present P(NIPAM-*co*-MAA) and PNIPAM systems, their chemical structures have no cis- or trans-configurations. Moreover, the DLS data in Figure 3 clearly show that the charged P(NIPAM-*co*-MAA) microgel exhibited a greater swelling capacity, so its structure is more loose, which makes it more difficult to form a confined space, compared with the neutral PNIPAM microgel. Therefore, considering that the biggest difference between the P(NIPAM-*co*-MAA) and PNIPAM microgels is their electrically charged characteristics, we speculate that the anomalous permittivity of P(NIPAM-*co*-MAA) microgel particles is related to the specific interactions within the polymer network. The charged ionic monomer MAA incured an extra ion-dipole interaction within the P(NIPAM-*co*-MAA) microgel,[59,60] and resulted in a larger

DOI: 10.1021/acs.macromol.6b00809
Macromolecules 2016, 49, 7997−8008

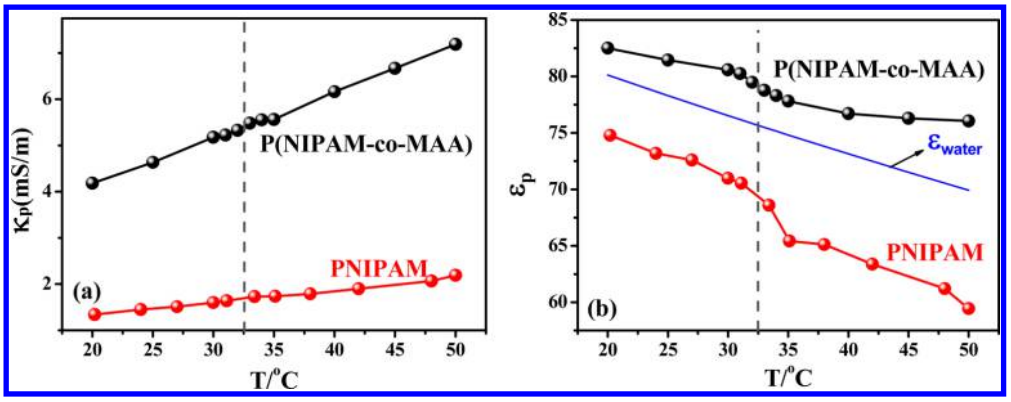

Figure 9. Temperature dependence of the (a) conductivity and (b) permittivity of two types of PNIPAM-based microgel particles. The VPTT is indicated by a dashed vertical line.

dipole moment. As a result, the P(NIPAM-*co*-MAA) microgel particles showed a high permittivity. An explanation for this at the molecular level is presented schematically in Figure 10. For

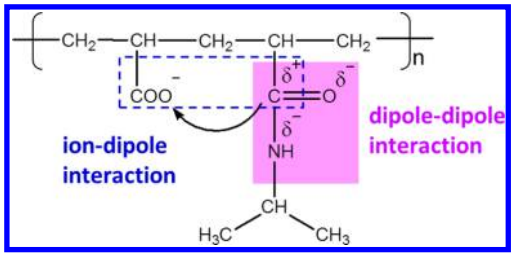

Figure 10. Schematic presentation of the specific interaction within the polymer network of P(NIPAM-*co*-MAA) microgels.

neutral PNIPAM microgel, its permittivity is only slightly less than that of water although the PNIPAM polymer matrix with very low permittivity is included. This is due to the permanent dipole moment of the side chain in NIPAM and the dipole−dipole interaction of hydrogen bond between the amide groups and water molecules (as shown by pink shaded area) contribute to the permittivity of PNIPAM microgel. However, for charged P(NIPAM-*co*-MAA) microgel, in addition to the contributions from the permanent dipole moment and hydrogen bond, there is an additional ion-dipole interaction between the carboxylate ions of MAA and the carbon atom of amide groups of NIPAM monomer (indicated by a blue box). Because the ion-dipole interaction is stronger than dipole−dipole interaction, the permittivity of the charged P(NIPAM-*co*-MAA) microgel is slightly larger than that of water. This result suggests that the polarity within the PNIPAM microgels will be increased by introducing the ionic monomers in the polymerizing procedure. And the particular importance of this finding is that it gave enough indications that this kind of material with stronger ion−dipole and dipole−dipole interaction may have potential applications in the controlled release of polar drugs[61]

3.4.2. Swelling Capacity and Dehydration Dynamics. In addition to the differences in the microgel structures, there are remarkable differences in their swelling capacity and dehydration dynamics between P(NIPAM-*co*-MAA) and PNIPAM microgels (The data of PNIPAM microgel are from ref 35). There are two parameters that are closely related to the swelling property, the size of microgels (see Figures 3 and 5) and the volume fraction (see Figure 11). It is clear from Figures 3, 5, and 11 that both the size and volume fraction of charged P(NIPAM-*co*-MAA) microgels are much bigger than those of

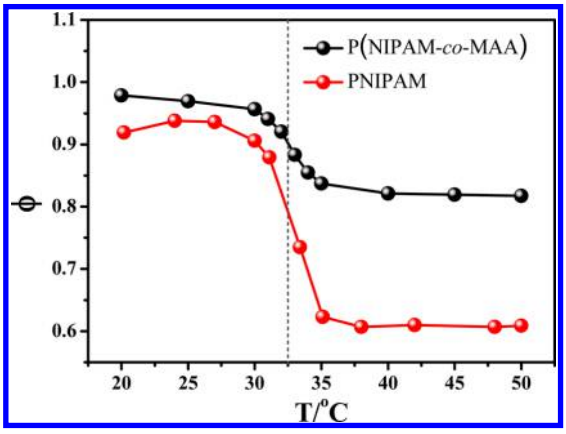

Figure 11. Temperature dependence of the volume fraction of two types of PNIPAM-based microgel particles.

neutral PNIPAM microgels at each temperature, which means that the swelling ability of PNIPAM-based microgels was increased greatly by introducing the ionic monomers. This result can be supported by the classical gel swelling theory proposed by Flory and Rehner.[26] According to the FR theory, the osmotic pressure Π for a gel to swell can be divided into three contributions:

$$\Pi = \Pi_{mix} + \Pi_{el} + \Pi_{ion} \quad (9)$$

Here Π_{mix}, Π_{el}, and Π_{ion} are the contributions come from mixing, deformation, and ion contributions, respectively. After introducing fixed charges to the network, the counterions have to be located near the fixed charges so as to keep the eletroneutrality. Therefore, introduction of ionic monomers of MAA into the gel network accommodates an additional osmotic contribution from ion/solvent mixing and electrostatic effects. As a result, water molecules will diffuse into the network, leading to an increase in swelling capacity of P(NIPAM-*co*-MAA) microgels, compared to PNIPAM microgels. Besides, Figure 10 also shows that as temperature increases, ϕ_{PNIPAM} reduces from 0.95 to 0.6, while $\phi_{PNIPAM\text{-}co\text{-}MAA}$ reduces from 0.97 to 0.85, indicating that the volume phase transition becomes less obvious for charged microgel. This also confirms the speculation in section 3.4.1 that the introduced polar charged groups will increase the rigidity of the network and hinder the collapse of microgel.

Furthermore, another difference for the two types of microgels is the continuity of volume phase transition. In other words, how did the charged groups affect the nature of

DOI: 10.1021/acs.macromol.6b00809
Macromolecules 2016, 49, 7997−8008

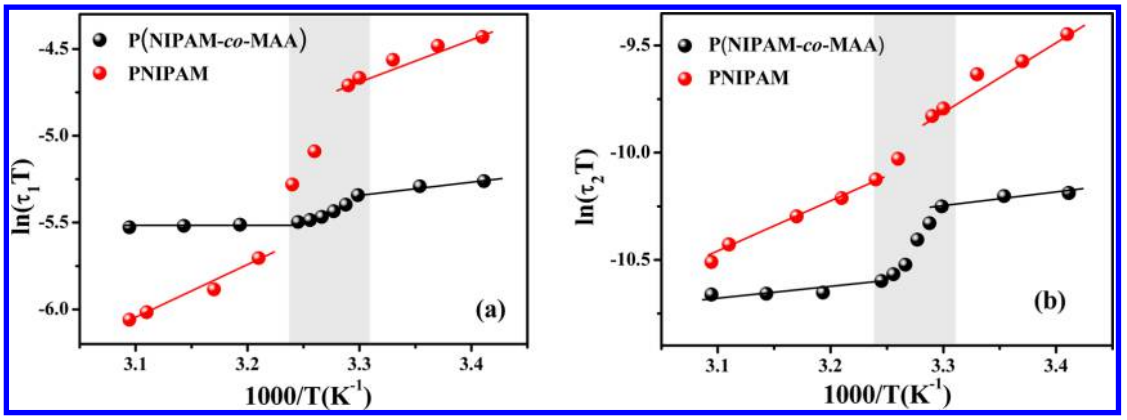

Figure 12. Eyring plots of the relaxation time of (a) low-frequency relaxation and (b) high-frequency relaxation for PNIPAM (red) and P(NIPAM-*co*-MAA) (black) microgel.

the volume phase transition? The answers were varied based on different research groups as mentioned in the Introduction. In this work, whether the DLS data or the results based on dielectric relaxation analysis, the changes of all the parameters for the charged P(NIPAM-*co*-MAA) microgels near the VPTT are less dramatic than those of neutral PNIPAM microgels. That means that the P(NIPAM-*co*-MAA) microgels have a less sharp phase transition, in comparison with that of PNIPAM microgels. This phenomenon is due to the delicate balance between the electrostatic repulsion of the carboxylate group of MAA and the hydrophobic attraction of NIPAM.

The volume phase transition of neutral PNIPAM microge results from the comprehensive effect of the hydrogen bonding and hydrophobic interaction. Below the VPTT, the PNIPAM microgels are in a highly swollen state in water due to the hydrogen bonding between the amide groups and water molecules, however, when the temperature is raised above the VPTT, the microgel collapses expelling most of its water due to the hydrophobic behavior of the pendent isopropyl groups as well as that of the backbone. When the ionic monomers of MAA were introduced into the neutral PNIPAM network, the repulsive electrostatic interactions between the fixed charges should be taken into account, which will further facilitate the swelling of microgels. When the temperature rises to the VPTT, for neutral PNIPAM microgels, the hydrogen bonding interaction became weak but hydrophobic interaction was enhanced instantaneously, resulting in a rapid and discontinuous volume phase transition. However, for the charged ionic P(NIPAM-*co*-MAA) microgels, although the electrostatic repulsion weakened in some degree due to the protonation of the carboxyl groups in MAA with decreasing pH in the process of arising temperature, it always can compete with the hydrophobic interaction of NIPAM; therefore, its volume phase transition is less sharper and more continuous.

3.4.3. Thermodynamics. We also found their differences in the thermodynamics properties between P(NIPAM-*co*-MAA) and PNIPAM microgels suspension by analyzing the temperature dependence of the relaxation time in Figure 6. The temperature dependence of τ was analyzed in terms of the Eyring equation:[62]

$$\ln(\tau T) = \ln\left(\frac{h}{k_B}\right) - \frac{\Delta S}{R} + \frac{\Delta H}{RT} \quad (10)$$

where h is Planck's constant, k_B is Boltzmann's constant, R is the universal gas constant, and ΔS and ΔH are the activation entropy and activation enthalpy, respectively.

The $\ln\tau T$ was plotted as a function of $1/T$ for both the low-frequency and high-frequency relaxation in Figure 12 (The data of PNIPAM microgel is from ref 35). Obviously, for P(NIPAM-*co*-MAA) and PNIPAM microgels, both of the two low- and high-frequency relaxation processes show a good linear relation between ln τT and $1/T$ below or above the VPTT, but are divided into two parts around the VPTT 32.5 °C, indicating a similar phase transition process. Furthermore, from the slop and the intercept of the fitting line, ΔH and ΔS of the two relaxations for the PNIPAM-based microgel particles were estimated and the results are listed in Table 4 and 5, respectively.

Table 4. Thermodynamic Parameters for the Low-Frequency Relaxation, Estimated by Eq 10

	ΔS(J·mol^{-1}·K^{-1})		ΔH(kJ·mol^{-1})	
sample	T < VPTT	T > VPTT	T < VPTT	T > VPTT
PNIPAM	−86.24	−79.49	21.96	21.92
P(NIPAM-*co*-MAA)	−133.69	−147.64	5.90	1.20

Table 5. Thermodynamic Parameters for the High-Frequency Relaxation, Estimated by Eq 10

	ΔS(J·mol^{-1}·K^{-1})		ΔH(kJ·mol^{-1})	
sample	T < VPTT	T > VPTT	T < VPTT	T > VPTT
PNIPAM	−44.67	−53.53	21.96	18.44
P(NIPAM-*co*-MAA)	−97.28	−106.67	4.57	0.67

Because these two dielectric relaxations are closely related to the hydrophilic-to-hydrophobic phase transition of the PNIPAM-based microgels, so as shown in Tables 4 and 5, the positive enthalpy ($\Delta H > 0$) and negative entropy ($\Delta S < 0$) indicated that the volume phase transition is an endothermic process, in which the microgels systems from a less ordered state to ordered one. It is also worth emphasizing that there is a big difference in the values of ΔH and ΔS between P(NIPAM-*co*-MAA) and PNIPAM microgels suspension. Here we focused on the activation entropy ΔS that connected with the degree of disorder of a system.

Figure 13 shows an example of the entropy change of the two PNIPAM-based microgel suspensions in low-frequency relax-

DOI: 10.1021/acs.macromol.6b00809
Macromolecules 2016, 49, 7997−8008

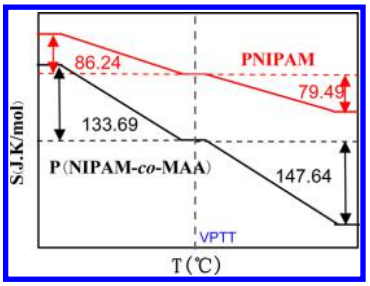

Figure 13. Entropy change diagram of PNIPAM (red) and P(NIPAM-*co*-MAA) (black) microgels suspension in the process of low-frequency relaxation.

ation process. We chose to discuss the low-frequency relaxation because it reflected the distribution of the counterions which determines partly the structure feature of a macromolecular and is an important issue in polyelectrolyte. For both of these two types of PNIPAM-based microgels, as can be seen in Figure 13, the activation entropy decreases with the increase of the temperature. When the microgels are in a highly swollen state (T < VPTT), the microgel particles and counterions are distributed heterogeneously in the whole suspension that result in the increase of the degree of disorder. With temperature increasing, the degree of disorder decreases due to the blocking/entrapping of counterions at the collapsed particles. In addition, due to the strong electrostatic interaction, the movement of the counterions is limited and the counterions fluctuate near the fixed charges within the polymer network. As a result, the degree of disorder of charged P(NIPAM-*co*-MAA) microgels suspension is a little less than that of neutral PNIPAM microgels in the whole temperature range.

In regard to the difference in ΔH between P(NIPAM-*co*-MAA) and PNIPAM microgels suspension, it was found that compared with neutral PNIPAM microgels, the ΔH values of the charged P(NIPAM-*co*-MAA) microgels suspension in the process of both the low- and high-frequency relaxation are smaller, indicating that the charged system needs relatively low energies to be polarized. This is because that the introduction of ionic monomers widened the difference of dielectric property between microgel particles and the aqueous medium as well as the concentration of the counterions, which are conducive to the counterion polarization and interfacial polarization.

4. CONCLUDING REMARKS

Dielectric behaviors of ionic P(NIPAM-*co*-MAA) microgels suspension have been systematically studied in a frequency range from 40 Hz to 110 MHz in the temperature range of 15 to 55 °C. Similar to neutral PNIPAM microgels reported recently, two remarkable and unique relaxation processes were clearly observed by successfully removing the electrode polarization, which will hopefully reflect the typical dielectric characteristics of the commonly cross-linked three-dimensional polymer network. However, the mechanisms of high-frequency relaxation of ionic P(NIPAM-*co*-MAA) microgels is significant different from that of PNIPAM microgels. This is due to the unique microstructure and properties of P(NIPAM-*co*-MAA) microgels. By systematically comparing the temperature dependences of relaxation mechanisms, dielectric parameters and phase parameters, we found that the introduction of charged groups has almost no effect on the volume phase transition temperature, but markedly affects the structure and dehydration dynamics of microgels. On the structure side, both the rigidity of polymer chain and the polarity within the P(NIPAM-*co*-MAA) microgels were increased. On the dehydration dynamics side, the introduction of ionic monomers into the microgel network accommodates an additional osmotic contribution from electrostatic effects, leading to a significant increase in swelling capacity and a continuous volume phase transition of P(NIPAM-*co*-MAA) microgels. Furthermore, the degree of disorder of P(NIPAM-*co*-MAA) microgels suspension was reduced due to the strong electrostatic interaction, which gave an image of the distribution of the counterions in a charged microgels.

In this work, the relation between the volume phase transition and charges groups in microgels was clarified. This work also provided a new insight into the structural evolution and dehydration dynamics of the copolymer microgels during phase transition. Besides, it implied that the dielectric analysis which is based on appropriate physical model is a promising tool to investigate the internal morphology and thermal behavior in thermally sensitive microgels system, offering reference and consulting for the dielectric research on the polyelectrolyte gels.

AUTHOR INFORMATION

Corresponding Author

*(K.Z.) Telephone: +86-010-58805856. E-mail: zhaoks@bnu.edu.cn.

Author Contributions

#W.S. and M.Y. contributed equally.

Notes

The authors declare no competing financial interest.

ACKNOWLEDGMENTS

This work was financially supported by the National Natural Scientific Foundation of China (Grant Nos. 21173025 and 21473012) and the Major Research Plan of NSFC (No.21233003).

REFERENCES

(1) Lim, H. L.; Hwang, Y.; Kar, M.; Varghese, S. Smart hydrogels as functional biomimetic systems. *Biomater. Sci.* **2014**, *2* (5), 603−618.

(2) Stuart, M. A. C.; Huck, W. T.; Genzer, J.; Müller, M.; Ober, C.; Stamm, M.; Sukhorukov, G. B.; Szleifer, I.; Tsukruk, V. V.; Urban, M.; et al. Emerging applications of stimuli-responsive polymer materials. *Nat. Mater.* **2010**, *9* (2), 101−113.

(3) Heskins, M.; Guillet, J. E. Solution properties of poly (N-isopropylacrylamide). *J. Macromol. Sci., Chem.* **1968**, *A2* (8), 1441−1455.

(4) Wu, C.; Zhou, S.; Au-yeung, S. C.; Jiang, S. Volume phase transition of spherical microgel particles. *Angew. Makromol. Chem.* **1996**, *240* (1), 123−136.

(5) Tanaka, T. Collapse of gels and the critical endpoint. *Phys. Rev. Lett.* **1978**, *40* (12), 820.

(6) Kojima, H.; Tanaka, F. Cooperative Hydration Induces Discontinuous Volume Phase Transition of Cross-Linked Poly (N-isopropylacrylamide) Gels in Water. *Macromolecules* **2010**, *43* (11), 5103−5113.

(7) Kokufuta, E.; Zhang, Y. Q.; Tanaka, T.; Mamada, A. Effects of surfactants on the phase transition of poly (N-isopropylacrylamide) gel. *Macromolecules* **1993**, *26* (5), 1053−1059.

(8) Sagle, L. B.; Zhang, Y.; Litosh, V. A.; Chen, X.; Cho, Y.; Cremer, P. S. Investigating the hydrogen-bonding model of urea denaturation. *J. Am. Chem. Soc.* **2009**, *131* (26), 9304−9310.

DOI: 10.1021/acs.macromol.6b00809
Macromolecules 2016, 49, 7997−8008

(9) Li, Y.; Tanaka, T. Phase transitions of gels. *Annu. Rev. Mater. Sci.* **1992**, *22* (1), 243−277.
(10) Zhang, Y.; Furyk, S.; Bergbreiter, D. E.; Cremer, P. S. Specific Ion Effects on the Water Solubility of Macromolecules: PNIPAM and the Hofmeister Series. *J. Am. Chem. Soc.* **2005**, *127* (41), 14505−14510.
(11) Zhang, Y.; Furyk, S.; Sagle, L. B.; Cho, Y.; Bergbreiter, D. E.; Cremer, P. S. Effects of Hofmeister Anions on the LCST of PNIPAM as a Function of Molecular Weight†. *J. Phys. Chem. C* **2007**, *111* (25), 8916−8924.
(12) Du, H.; Wickramasinghe, R.; Qian, X. Effects of salt on the lower critical solution temperature of poly (N-isopropylacrylamide). *J. Phys. Chem. B* **2010**, *114* (49), 16594−16604.
(13) Lee, L.-T.; Cabane, B. Effects of surfactants on thermally collapsed poly (N-isopropylacrylamide) macromolecules. *Macromolecules* **1997**, *30* (21), 6559−6566.
(14) Richter, M.; Zakrevskyy, Y.; Eisele, M.; Lomadze, N.; Santer, S.; Klitzing, R. v. Effect of pH, co-monomer content, and surfactant structure on the swelling behavior of microgel-azobenzene-containing surfactant complex. *Polymer* **2014**, *55* (25), 6513−6518.
(15) Reddy, P. M.; Venkatesu, P. Ionic Liquid Modifies the Lower Critical Solution Temperature (LCST) of Poly(N-isopropylacrylamide) in Aqueous Solution. *J. Phys. Chem. B* **2011**, *115* (16), 4752−4757.
(16) Reddy, P. M.; Umapathi, R.; Venkatesu, P. Interactions of ionic liquids with hydration layer of poly(N-isopropylacrylamide): comprehensive analysis of biophysical techniques results. *Phys. Chem. Chem. Phys.* **2014**, *16* (22), 10708−10718.
(17) Chang, C.-J.; Reddy, P. M.; Hsieh, S.-R.; Huang, H.-C. Influence of imidazolium based green solvents on volume phase transition temperature of crosslinked poly(N-isopropylacrylamide-co-acrylic acid) hydrogel. *Soft Matter* **2015**, *11* (4), 785−792.
(18) Zhang, G.; Wu, C. The Water/Methanol Complexation Induced Reentrant Coil-to-Globule-to-Coil Transition of Individual Homopolymer Chains in Extremely Dilute Solution. *J. Am. Chem. Soc.* **2001**, *123* (7), 1376−1380.
(19) Scherzinger, C.; Schwarz, A.; Bardow, A.; Leonhard, K.; Richtering, W. Cononsolvency of poly-N-isopropyl acrylamide (PNIPAM): Microgels versus linear chains and macrogels. *Curr. Opin. Colloid Interface Sci.* **2014**, *19* (2), 84−94.
(20) Gao, Y.; Yang, J.; Ding, Y.; Ye, X. Effect of Urea on Phase Transition of Poly(N-isopropylacrylamide) Investigated by Differential Scanning Calorimetry. *J. Phys. Chem. B* **2014**, *118* (31), 9460−9466.
(21) Sun, S.; Hu, j.; Tang, H.; Wu, P. Spectral interpretation of thermally irreversible recovery of poly(N-isopropylacrylamide-co-acrylic acid) hydrogel. *Phys. Chem. Chem. Phys.* **2011**, *13* (11), 5061−5067.
(22) Hirose, H.; Shibayama, M. Kinetics of volume phase transition in poly (N-isopropylacrylamide-co-acrylic acid) gels. *Macromolecules* **1998**, *31* (16), 5336−5342.
(23) Kratz, K.; Hellweg, T.; Eimer, W. Influence of charge density on the swelling of colloidal poly(N-isopropylacrylamide-co-acrylic acid) microgels. *Colloids Surf., A* **2000**, *170* (2−3), 137−149.
(24) Ye, Y.; Shangguan, Y.; Song, Y.; Zheng, Q. Influence of charge density on rheological properties and dehydration dynamics of weakly charged poly(N-isopropylacrylamide) during phase transition. *Polymer* **2014**, *55* (10), 2445−2454.
(25) Ilmain, F.; Tanaka, T.; Kokufuta, E. Volume transition in a gel driven by hydrogen bonding. *Nature* **1991**, *349* (6308), 400−401.
(26) Quesada-Perez, M.; Maroto-Centeno, J. A.; Forcada, J.; Hidalgo-Alvarez, R. Gel swelling theories: the classical formalism and recent approaches. *Soft Matter* **2011**, *7* (22), 10536−10547.
(27) Hirotsu, S.; Hirokawa, Y.; Tanaka, T. Volume-phase transitions of ionized N-isopropylacrylamide gels. *J. Chem. Phys.* **1987**, *87*, 1392.
(28) Shibayama, M.; Mizutani, S.-y.; Nomura, S. Thermal properties of copolymer gels containing N-isopropylacrylamide. *Macromolecules* **1996**, *29* (6), 2019−2024.
(29) Beltran, S.; Baker, J. P.; Hooper, H. H.; Blanch, H. W.; Prausnitz, J. M. Swelling equilibria for weakly ionizable, temperature-sensitive hydrogels. *Macromolecules* **1991**, *24* (2), 549−551.
(30) Fernández-Nieves, A.; Fernández-Barbero, A.; Vincent, B.; de las Nieves, F. J. Charge Controlled Swelling of Microgel Particles. *Macromolecules* **2000**, *33* (6), 2114−2118.
(31) Masci, G.; Cametti, C. Dielectric properties of thermo-reversible hydrogels: the case of a dextran copolymer grafted with poly (N-isopropylacrylamide). *J. Phys. Chem. B* **2009**, *113* (33), 11421−11428.
(32) Gómez-Galván, F.; Lara-Ceniceros, T.; Mercado-Uribe, H. Device for simultaneous measurements of the optical and dielectric properties of hydrogels. *Meas. Sci. Technol.* **2012**, *23* (2), 025602.
(33) Zhou, J.; Wei, J.; Ngai, T.; Wang, L.; Zhu, D.; Shen, J. Correlation between Dielectric/Electric Properties and Cross-Linking/Charge Density Distributions of Thermally Sensitive Spherical PNIPAM Microgels. *Macromolecules* **2012**, *45* (15), 6158−6167.
(34) Füllbrandt, M.; von Klitzing, R.; Schönhals, A. The dielectric signature of poly (N-isopropylacrylamide) microgels at the volume phase transition: dependence on the crosslinking density. *Soft Matter* **2013**, *9* (17), 4464−4471.
(35) Su, W.; Zhao, K.; Wei, J.; Ngai, T. Dielectric relaxations of poly(N-isopropylacrylamide) microgels near the volume phase transition temperature: impact of cross-linking density distribution on the volume phase transition. *Soft Matter* **2014**, *10* (43), 8711−8723.
(36) Wei, J.; Li, Y.; Ngai, T. Tailor-made microgel particles: Synthesis and characterization. *Colloids Surf., A* **2016**, *489*, 122−127.
(37) Schwan, H. *Physical techniques in biological research*; Academic: New York, 1963; Vol. *6*, p 373.
(38) Asami, K.; Irimajiri, A.; Hanai, T.; Koizumi, N. A method for estimating residual inductance in high frequency AC measurements. *Bull. Inst. Chem. Res., Kyoto Univ.* **1973**, *51*, 231−245.
(39) Van Beek, L. Dielectric behaviour of heterogeneous systems. *Prog. Dielectrics* **1967**, *7*, 69−114.
(40) Havriliak, S.; Negami, S. A complex plane representation of dielectric and mechanical relaxation processes in some polymers. *Polymer* **1967**, *8*, 161−210.
(41) Jiménez, M.; Arroyo, F.; van Turnhout, J.; Delgado, A. V. Analysis of the dielectric permittivity of suspensions by means of the logarithmic derivative of its real part. *J. Colloid Interface Sci.* **2002**, *249* (2), 327−335.
(42) Wübbenhorst, M.; van Turnhout, J. Analysis of complex dielectric spectra. I. One-dimensional derivative techniques and three-dimensional modelling. *J. Non-Cryst. Solids* **2002**, *305* (1), 40−49.
(43) Grosse, C.; Delgado, A. Dielectric dispersion in aqueous colloidal systems. *Curr. Opin. Colloid Interface Sci.* **2010**, *15* (3), 145−159.
(44) Lide, D. R. *CRC Handbook of Chemistry and Physics*; CRC Press: Boca Raton, FL, 2000; pp 5−93.
(45) Dukhin, S. S. Electrochemical characterization of the surface of a small particle and nonequilibrium electric surface phenomena. *Adv. Colloid Interface Sci.* **1995**, *61*, 17−49.
(46) Ito, K.; Yagi, A.; Ookubo, N.; Hayakawa, R. Crossover behavior in high-frequency dielectric relaxation of linear polyions in dilute and semidilute solutions. *Macromolecules* **1990**, *23* (3), 857−862.
(47) Furusawa, H.; Ito, K.; Hayakawa, R. High-frequency dielectric relaxation of polyelectrolyte gels. *Phys. Rev. E: Stat. Phys., Plasmas, Fluids, Relat. Interdiscip. Top.* **1997**, *55* (55), 7283−7287.
(48) Takashima, S. *Electrical Properties of Biopolymers and Membranes*; A. Hilger: 1989.
(49) Nakano, S.; Sato, Y.; Kita, R.; Shinyashiki, N.; Yagihara, S.; Sudo, S.; Yoneyama, M. Molecular Dynamics of Poly (N-isopropylacrylamide) in Protic and Aprotic Solvents Studied by Dielectric Relaxation Spectroscopy. *J. Phys. Chem. B* **2012**, *116* (2), 775−781.
(50) Füllbrandt, M.; Ermilova, E.; Asadujjaman, A.; Hölzel, R.; Bier, F. F.; von Klitzing, R.; Schönhals, A. Dynamics of Linear Poly(N-isopropylacrylamide) in Water around the Phase Transition

DOI: 10.1021/acs.macromol.6b00809
Macromolecules 2016, 49, 7997−8008

Investigated by Dielectric Relaxation Spectroscopy. *J. Phys. Chem. B* **2014**, *118* (13), 3750−3759.
(51) Ono, Y.; Shikata, T. Contrary hydration behavior of N-isopropylacrylamide to its polymer, P (NIPAm), with a lower critical solution temperature. *J. Phys. Chem. B* **2007**, *111* (7), 1511−1513.
(52) Hanai, T. Theory of the dielectric dispersion due to the interfacial polarization and its application to emulsions. *Colloid Polym. Sci.* **1960**, *171* (1), 23−31.
(53) Hanai, T.; Sherman, P. *Emulsion Science*; Academic Press: New York, 1968; p 353.
(54) Lide, D. R. *CRC Handbook of Chemistry and Physics*; CRC Press: Boca Raton, FL, 2000; pp 6−139.
(55) Yılmaz, Y.; Gelir, A.; Salehli, F.; Nigmatullin, R.; Arbuzov, A. Dielectric study of neutral and charged hydrogels during the swelling process. *J. Chem. Phys.* **2006**, *125* (23), 234705.
(56) Rubinstein, M.; Colby, R. H. *Polymer physics*. OUP: Oxford, U.K., 2003; p pp 49−51.
(57) Ballenegger, V.; Hansen, J.-P. Dielectric permittivity profiles of confined polar fluids. *J. Chem. Phys.* **2005**, *122* (11), 114711.
(58) Banys, J.; Kinka, M.; Macutkevic, J.; Völkel, G.; Böhlmann, W.; Umamaheswari, V.; Hartmann, M.; Pöppl, A. Broadband dielectric spectroscopy of water confined in MCM-41 molecular sieve materials—low-temperature freezing phenomena. *J. Phys.: Condens. Matter* **2005**, *17* (19), 2843.
(59) Krygowski, T.; Fawcett, W. Complementary Lewis acid-base description of solvent effects. I. Ion-ion and ion-dipole interactions. *J. Am. Chem. Soc.* **1975**, *97* (8), 2143−2148.
(60) Kashyap, H. K.; Biswas, R. Solvation Dynamics of Dipolar Probes in Dipolar Room Temperature Ionic Liquids: Separation of Ion− Dipole and Dipole− Dipole Interaction Contributions. *J. Phys. Chem. B* **2010**, *114* (1), 254−268.
(61) Ward, M. A.; Georgiou, T. K. Thermoresponsive polymers for biomedical applications. *Polymers* **2011**, *3* (3), 1215−1242.
(62) Davies, M.; Swain, J. Dielectric studies of configurational changes in cyclohexane and thianthrene structures. *Trans. Faraday Soc.* **1971**, *67*, 1637−1653.

DOI: 10.1021/acs.macromol.6b00809
Macromolecules 2016, 49, 7997−8008